HHS Public Access

Author manuscript

Eur Radiol. Author manuscript; available in PMC 2020 January 01.

Published in final edited form as:

Eur Radiol. 2019 January ; 29(1): 458–467. doi:10.1007/s00330-018-5542-8.

Quantitative imaging features of pre-treatment CT predict volumetric response to chemotherapy in patients with colorectal liver metastases

John M. Creasy, MD[1], **Abhishek Midya, PhD**[1], **Jayasree Chakraborty, PhD**[1], **Lauryn B. Adams, BA**[1], **Camilla Gomes, BA**[1], **Mithat Gonen, PhD**[5], **Kenneth P. Seastedt, MD**[1], **Elizabeth J. Sutton, MD**[2], **Andrea Cercek, MD**[3], **Nancy E. Kemeny, MD**[3], **Jinru Shia, MD**[4], **Vinod P. Balachandran, MD**[1], **T. Peter Kingham, MD**[1], **Peter J. Allen, MD**[1], **Ronald P. DeMatteo, MD**[1], **William R. Jarnagin, MD**[1], **Michael I. D'Angelica, MD**[1], **Richard K.G. Do, MD, PhD**[2], and **Amber L. Simpson, PhD**[1]

[1]Department of Surgery, Memorial Sloan Kettering Cancer Center, New York, NY

[2]Department of Radiology, Memorial Sloan Kettering Cancer Center, New York, NY

[3]Department of Medicine, Memorial Sloan Kettering Cancer Center, New York, NY

[4]Department of Pathology, Memorial Sloan Kettering Cancer Center, New York, NY

[5]Department of Epidemiology and Biostatistics, Memorial Sloan Kettering Cancer Center, New York, NY

Abstract

Objective: This study investigates whether quantitative image analysis of pre-treatment CT scans can predict volumetric response to chemotherapy for patients with colorectal liver metastases (CRLM).

Corresponding Author: Amber Simpson, PhD, Assistant Attending Computational Biologist, Hepatopancreatobiliary Service, Department of Surgery, 1275 York Avenue, C-891, New York, NY 10065, simpsonl@mskcc.org.

Guarantor:
The scientific guarantor of this publication is Amber L. Simpson, PhD.

Conflict of interest:
The authors of this manuscript declare no relationships with any companies, whose products or services may be related to the subject matter of the article.

Statistics and biometry:
Mithat Gonen, PhD kindly provided statistical advice for this manuscript.

Informed consent:
Written informed consent was waived by the Institutional Review Board.

Ethical approval:
Institutional Review Board approval was obtained.

Methodology:

- retrospective
- experimental
- performed at one institution

Methods: Patients treated with chemotherapy for CRLM (hepatic artery infusion (HAI) combined with systemic or systemic alone) were included in the study. Patients were imaged at baseline and approximately 8 weeks after treatment. Response was measured as the percentage change in tumor volume from baseline. Quantitative imaging features were derived from the index hepatic tumor on pre-treatment CT, and features statistically significant on univariate analysis were included in a linear regression model to predict volumetric response. The regression model was constructed from 70% of data, while 30% were reserved for testing. Test data were input into the trained model. Model performance was evaluated with mean absolute prediction error (MAPE) and R^2. Clinicopathololgic factors were assessed for correlation with response.

Results: 157 patients were included, split into training (n=110) and validation (n=47) sets. MAPE from the multivariate linear regression model was 16.5% (R^2=0.774) and 21.5% in the training and validation sets, respectively. Stratified by HAI utilization, MAPE in the validation set was 19.6% for HAI and 25.1% for systemic chemotherapy alone. Clinical factors associated with differences in median tumor response were treatment strategy, systemic chemotherapy regimen, age, and KRAS mutation status ($p<0.05$).

Conclusion: Quantitative imaging features extracted from pre-treatment CT are promising predictors of volumetric response to chemotherapy in patients with CRLM. Pre-treatment predictors of response have the potential to better select patients for specific treatments.

Keywords

1. Colorectal neoplasms; 2. Multidetector computed tomography; 3. Liver; 4. Prognosis; 5. Models, Statistical

Introduction

With nearly 140,000 new cases annually, colorectal cancer is the second leading cause of cancer-related mortality in the United States.[1, 2] The liver remains the most common site of metastasis and <5% of patients with colorectal liver metastases (CRLM) survive past five years if untreated.[3–6] Combinations of systemic and regional therapies have been utilized to downsize CRLM, and in patients selected for hepatic resection, up to 20% can be cured.[7; 8] However, there is currently no method to *predict* response prior to chemotherapy administration for patients with CRLM. Identification of patients most or least likely to respond to a specific modality would allow a targeted approach to downsizing CRLM and tailored selection of treatments. In current clinical practice, response to chemotherapy is evaluated with radiographic criteria assessed on images obtained pre- and post-treatment (i.e. Response Evaluation Criteria in Solid Tumors [RECIST]).[9] Studies have explored imaging predictors of response with tumor morphology, early tumor shrinkage, perfusion CT, and MRI, but these approaches require specialized sequences or analyze tumor change between two distinct points in time, after initiation of treatment.[10–16] Thus, validated pre-treatment predictors of tumor response are needed to optimize the management of CRLM.

Since contrast-enhanced CT scans are routinely obtained for staging in colorectal cancer patients, they are widely available for image analysis and biomarker development.[17–19] Radiomics is an emerging field in which medical images are converted into mineable data by

automated extraction of quantitative features that represent changes in radiographic enhancement patterns.[20] By applying radiomics to solid malignancies, imaging features can provide quantification of tumoral heterogeneity that is related to cell-density, necrosis, fibrosis and hemorrhage.[21] Quantitative image analysis on CT scans has demonstrated an association between tumoral heterogeneity and survival in primary colorectal cancers and CRLM where patients with more heterogeneous tumors tended to have improved outcomes.[21; 22] Based on this finding, we sought to predict response to chemotherapy with quantitative image analysis of routine CT scans.

The main objective of our study is to evaluate whether imaging features from a single pre-treatment CT scan can be used to predict volumetric response for patients receiving chemotherapy for CRLM.

Patients and Methods

Patients

Approval from the Institutional Review Board was obtained for retrospective analysis with waiver of informed consent. The study population was pooled from A) two previously published prospective trials evaluating hepatic artery infusion (HAI) plus systemic chemotherapy for unresectable CRLM[23; 24] and B) patients from a consecutive series from 2003 to 2007 previously reported on the use of neoadjuvant chemotherapy prior to hepatic resection.[25] Data Supplement 1 includes full inclusion and exclusion criteria: patients were excluded if they did not undergo a portal venous phase CT or receive the intended chemotherapy within each respective cohort. Inclusion in HAI trials required that patients have no evidence of extrahepatic metastases and be deemed to have unresectable CRLM by a multidisciplinary group of hepatobiliary surgeons and radiologists. In the second trial, the definition of unresectable CRLM was refined to include both technical (margin-negative resection would require resection of both portal veins, 3 hepatic veins, or the retrohepatic vena cava or resection would leave < 2 adequately perfused and drained segments) or biologic (>6 metastases in a single lobe, with 1 lesion ≥5cm or ≥6 bilobar metastases) considerations.

Additional clinical and laboratory variables were collected from the electronic medical record and a prospectively maintained Hepatopancreatobiliary Service database within our institution. Synchronous disease was defined as hepatic metastases within 6 months of primary colon cancer diagnosis. Clinical risk score (CRS) has been previously reported and is comprised of five factors: greater than 1 tumor, tumor greater than 5 cm, carcinoembryonic antigen (CEA) greater than 200 ng/mL, lymph node positive primary, and disease free interval less than 12 months.[26] CRS was dichotomized into low (0–2) and high (3–5) risk groups.

Chemotherapy Regimens

Cohort A was assembled from two previous clinical trials in which patients received standard HAI pump placement and infusion of floxuridine/dexamethasone (HAI FUDR) in combination with systemic chemotherapy.[27] Cohort A included patients that had received

previous systemic chemotherapy and those that were treatment naïve. All patients received HAI FUDR, but systemic chemotherapy varied by protocol, including irinotecan in all instances and oxaliplatin based on previous oxaliplatin utilization.[23; 24] Bevacizumab was administered to approximately half of the patients in the latter protocol.

Patients from Cohort B received first-line systemic neoadjuvant chemotherapy prior to hepatic resection. No patient in Cohort B had received systemic chemotherapy within the previous year at the time of pre-treatment imaging. Treatment regimens were not standardized and administered at the discretion of the primary medical oncologist. Various first-line combinations were employed, but included either oxaliplatin or irinotecan in all instances. Bevacizumab was selectively utilized.

For comparison of clinical factors associated with response, patients were grouped based on the three overall treatment strategies included in this study: HAI in chemotherapy naïve, HAI in previously treated patients, and first-line systemic chemotherapy in treatment naïve patients. Systemic chemotherapy regimen was defined as the specific combination of systemic treatment, irrespective of HAI utilization, administered to the patient during the study interval.

Study Design, CT Imaging, and Statistical Analysis

Chemotherapy response was measured as the percentage volumetric change of the index hepatic metastasis from baseline to the first follow-up CT scan obtained at approximately 8 weeks. The index hepatic metastasis was defined as the largest lesion that could be followed on repeat imaging in accordance with RECIST guidelines. Routine contrast-enhanced portal venous phase CT was used in all measurements. Multidetector CT scanner (Lightspeed 16 and VCT, GE Healthcare) was employed for abdominal imaging with main parameters: autoMA 220–380; noise index 12–14; rotation time 0.7–0.8 milliseconds; scan delay 80 seconds. Images for selected patients were transferred from the picture archiving and communication system (PACS) to a workstation for image processing. The liver, tumors, vessels, and bile ducts were semi-automatically segmented by using Scout Liver (Pathfinder Technologies Inc.) and a 3D model generated. An image volume was created with the index tumor from the pre- and post-treatment scans.

Amongst all patients, clinicopathologic variables were assessed for an association with median percent volumetric response and evaluated using the Mann-Whitney U test or Kruskal-Wallis test where appropriate. Differences in patient characteristics between training and validation sets were compared using Fisher exact test or chi-square test depending on the number of observations. A p-value less than 0.05 was considered statistically significant and 95% confidence intervals were used. Analyses were conducted using SPSS statistical software (Version 22.0).

Quantitative Image Analysis

Quantitative image analysis was performed on the index tumor on baseline CT. A set of 272 imaging features, representing heterogeneity, were extracted using gray-level co-occurrence matrices (GLCM), run-length matrices (RLM), local binary patterns (LBP), fractal dimension (FD), intensity histogram (IH), and angle co-occurrence matrices (ACMs).[28–

42] Data Supplement 2 further describes feature extraction and image analysis, and Data Supplement 3 lists all imaging features included in this study.

Prediction Model Building & Validation

Cohort A and B patients were combined and randomly split into training and validation sets, stratified by HAI to ensure proportional distribution of treatment strategies. Seventy percent of data (n=110) were used to build the prediction model, and 30% of data (n=47) were reserved for validation. Based on univariate analysis, quantitative imaging features associated with tumor response with p-value <0.05 were initially selected. Highly correlated imaging features (correlation coefficient >0.75) were removed from the feature set. In the situation of two highly correlated variables, only the imaging feature with the strongest association with response was retained. The remaining features and a variable denoting HAI utilization were included in the final multivariate linear regression. Prediction error was reported as the mean absolute prediction error (MAPE), computed as the absolute difference between actual and predicted percent response, for both training and validation data. Figure 1 demonstrates workflow for image segmentation, feature extraction and selection, model building, and evaluation.

Results

Patient Characteristics

In total, 157 patients were pooled from Cohort A (n=103) and Cohort B (n=54) for quantitative image analysis to predict volumetric response. Clinicopathologic factors of all patients and the actual volumetric response are listed in Table 1a. Representative of the advanced stage and unresectable nature of many patients, the majority had bilobar disease (84%) and multiple lesions (90%). Overall, 43 patients (27%) were chemotherapy naïve and received HAI and systemic therapy, 60 patients (38%) received HAI after prior systemic treatment, and 54 patients (34%) received systemic chemotherapy only without previous treatment. After randomly splitting the data into training and validation sets, Table 1b displays the distribution of clinicopathologic factors among patients in the respective groups. The only significant difference between the training and validation sets were a greater proportion of patients in the latter with CEA >200 (36% vs 19%, p=0.025).

Clinical Factors Related to Volumetric Response

Table 1a demonstrates the association of clinical factors and volumetric response. Among all patients, median percent volumetric change was −68% (range −100 to +193%). Median percent volumetric change was significantly different stratified by age, overall treatment strategy, systemic chemotherapy regimen, bevacizumab administration, and KRAS mutational status (p=0.001–0.007). Patients who were initially treatment naïve and received HAI and systemic chemotherapy had the largest median tumor response. Indicative of trial participants with HAI and limited previous treatment, patients that received systemic oxaliplatin and irinotecan had the largest median response among systemic chemotherapy regimens. Patients with mutant KRAS had a decreased median volumetric response compared to those with wild-type or unknown mutational status. There were no associations

between volumetric response and gender, colon or rectal primary, synchronous or bilobar disease, multiple lesions, tumor >5cm, node-positive primary, CEA >200, or CRS ($p>0.05$).

Feature Selection Results

Quantitative imaging features were evaluated for their association with response. Based on the univariate analysis and correlation coefficients, 30 features from the CT images in the training set were selected as inputs for the final multivariate regression model, Table 2. In Figure 2, one of the most predictive imaging features, called entropy, was chosen to illustrate CT appearance differences among patients with varying volumetric responses. Entropy is a commonly evaluated feature in the literature that describes pixel randomness within a grayscale image.[22] Higher entropy values, representing increased heterogeneity, were associated with increased volumetric response in CRLM.[43; 44] Representative CT images, 24×24 pixel patches from the index tumor, entropy values, and responses are depicted in Figure 2. Entropy was calculated using the entire tumor volume.

Creation and Evaluation of Prediction Model

Combining the selected features from the training set, a multivariate linear regression was constructed for percentage tumor response. This prediction model was then separately tested with the same features extracted from the CT images in the validation cohort. The training and validation results of the regression models are listed in Table 3. MAPE represents the mean difference between the predicted responses from the model versus the actual radiographic responses. The MAPE for the training set was 16.5%, and for the validation set, 21.5%. R^2 value for the regression was 0.77. Figure 3a and 3b include scatterplots of predicted versus actual response for training and validation sets. A waterfall plot of prediction error for all training as well as test cases is provided in Figure 3c to illustrate the distribution of error over different samples. A secondary analysis of the patients in the validation set, stratified by HAI utilization, demonstrated a MAPE of 19.5% (n=31) for those patients with HAI chemotherapy and 25.1% (n=16) for patients with systemic chemotherapy only.

Discussion

For patients with CRLM treated with chemotherapy, pre-treatment CT image analysis contains predictive information for early response as measured by volumetric change. The magnitude of response of CRLM was also associated with overall treatment strategy, the type of systemic chemotherapy, age, and KRAS mutation status. This is the first study to predict volumetric treatment response using tumor-derived quantitative features of heterogeneity from routinely acquired pre-treatment CT scans. These results represent a step in the development of radiomics for clinical applications to improve selection of specific treatments for patients with CRLM.

Predicting response based on tumor enhancement patterns on a pre-treatment CT has clinical utility for all patients with CRLM. Radiographic response to chemotherapy will have different implications based on individual clinical scenario, but a pre-treatment prediction would be a tool for any oncologist or surgeon who treats patients with CRLM. Thus, we

included patients with initially unresectable and resectable metastatic disease, distributed evenly between the 70/30 training and validation sets. In the validation set, we observed a MAPE of 21.5%, which represents the mean error between the predicted response and the actual radiographic response. To determine whether the achieved error (21.5%) was clinically acceptable, the tumor was modeled as a sphere. The majority of the volume of a sphere lies at the surface. Considering the tumor as a sphere, the error in the radius is less than 8%. This means that in a tumor with a change in radius of 10 mm, we would predict a tumor radius change of 9.2 mm or 10.7 mm. The error is therefore within the bounds of CT scanner resolution and segmentation accuracy. As a true radiographic prediction from one distinct time point, the model displays acceptable error with a high R^2 value. At present, this model may have the most utility at the extremes of response. Pre-treatment identification of patients with a very favorable or unfavorable response to treatment would assist clinical decision-making.

Compared to previous studies, our approach addresses the limitation of using specialized imaging techniques or multiple imaging time points to predict response in CRLM. Kim et al. identified changes in CT perfusion parameters as predictors of early tumor response using the pre-treatment and first post-treatment scan.[13] Early tumor shrinkage (ETS) of target lesions is also associated with outcomes, but both of these techniques give prognostic information only after the first cycle of chemotherapy.[11] Other groups have investigated baseline dynamic contrast-enhanced MRI to predict treatment outcome, but this requires imaging studies not performed in routine staging of metastatic colorectal cancer.[15] Our results demonstrate that quantitative image analysis of one routinely acquired pre-treatment CT scan holds information predictive of early response. This process may be automated in the future, and if validated, more widely applicable to general practice due to the ubiquitous use of contrast-enhanced CT.

Similar to radiographic CRLM morphology, our group hypothesized that there is a relationship between tumor heterogeneity on quantitative imaging and response.[10] The Hounsfield unit (HU) is a standard measure in CT scanning that reflects the overall atomic density of soft tissues being imaged. The density of CRLM will vary across patients by their differential uptake of iodinated contrast on contrast-enhanced CT. While each imaging feature of heterogeneity is weighted differently, 30 individual features served as inputs for the regression model. Entropy, a measure of the randomness of pixel intensity values within a region of interest, was one of the selected features for the model. Entropy is discriminatory in the literature and also can be well described in radiographic terms. For illustration purposes, entropy and representative pre- and post-treatment CT scans were shown in Figure 2. Entropy showed an association between higher values and increased response. Heterogeneous tumors, with higher entropy, may exhibit improved vascular delivery of chemotherapy and viable tumor tissue. Heterogeneous tumors have already been associated with improved survival [22], but our results support the hypothesis that tumors with increased heterogeneity also have greater potential for volumetric response to chemotherapy.

Currently, HAI chemotherapy is restricted to a small group of high-volume centers. HAI has been shown to be most efficient when used as first-line therapy.[45] In our study, the greatest median response was observed in patients treated with HAI and systemic chemotherapy who

were chemotherapy naïve. Prior chemotherapy had been administered to a subset of HAI patients (n=60) in this analysis. Decreased volumetric response was expected in this group based on published rates of response with HAI in patients with prior chemotherapy versus chemotherapy-naïve.[24; 46] Nonetheless, a median volumetric response of 61% demonstrates the impact of HAI, especially in a previously treated population. For this reason, HAI utilization was included as a variable in the prediction model. An accurate pre-treatment, radiographic predictor of response would allow better patient selection for HAI therapy. The potential clinical benefit is two-fold, avoiding HAI pump placement in patients with predicted marginal benefit, but also increasing utilization in patients with predictably favorable responses. At present, HAI pump chemotherapy is an expensive treatment with potential complications that demands close patient and physician involvement and commitment.[47] Developing predictors of response will aid patients in making informed decisions regarding their choice of specific treatments.

Since the use of HAI remains limited, we also included patients who were treated with systemic chemotherapy alone. In previous systemic chemotherapy studies, partial response was observed in 28–72% of patients.[7] Our results demonstrate that the median volumetric change was −66% in this subset, but the results are spread over a wide range (−100% to +193%). As first-line systemic chemotherapy in previously untreated patients, these findings are not surprising. Nonetheless, this study was not designed to directly compare different treatment strategies or make chemotherapy recommendations; rather, the project was aimed at building a prediction model based on CT enhancement patterns of pre-treatment CRLM, regardless of therapy. By incorporating patients in the training set with a wide range of treatments and responses, the prediction model was created with image analysis of CT scans from a population that reflects the variation encountered in actual clinical practice.

This study has several limitations. First, this was a retrospective study and these results are limited to patients at a tertiary center with high-volume HAI pump placement and hepatic resections. Second, this study only analyzed the index tumor. In CRLM, individual hepatic metastases may potentially show different volumetric responses to chemotherapy. However, given the varied number of hepatic metastases between patients, considerations regarding statistical analysis and the regression model influenced our decision to include only the index hepatic tumor. Furthermore, other clinical variables, such as KRAS mutation status, are important but not captured by quantitative imaging. Patients with KRAS mutation show decreased volumetric response (55% vs 74% median volumetric response) in our dataset. This mutational data was only available for 64% of patients (100/157). KRAS mutations have already been shown to independently predict pathologic response in resected CRLM.[48] Since KRAS mutation status may not be known at the time of CRLM diagnosis, it was not included in the prediction model. As next-generation sequencing improves, these results indicate the future potential to combine both pre-treatment CT imaging and genomic variables to predict response with a high degree of accuracy. Even with these limitations, this study linked quantitative imaging features with clinically applicable data from prospective trials and a retrospective surgical series. The next steps in development include validation of these methods with a separate dataset from another institution or ideally a prospective trial of quantitative image analysis and response. Further prospective investigations accounting

for type and delivery of chemotherapy may allow improved prediction models with the potential to better select patients for specific treatments.

Conclusion

This study demonstrates that quantitative imaging features extracted from pre-treatment CT are promising predictors of volumetric response to chemotherapy in patients with CRLM. Prospective validation is required prior to using these novel imaging markers in the clinical setting, but should be pursued. Pre-treatment prediction of response to chemotherapy has the potential to better select patients for individualized treatments.

Supplementary Material

Refer to Web version on PubMed Central for supplementary material.

Acknowledgments

Funding:

This study has received funding by NIH/NCI P30 CA008748 Cancer Center Support Grant and the Society for Memorial Sloan Kettering.

Abbreviations:

ACM	angle co-occurrence matrix
CEA	carcinoembryonic antigen
CRLM	colorectal liver metastases
CRS	clinical risk score
ETS	early tumor shrinkage
FD	fractal dimension
FUDR	floxuridine
GLCM	gray-level co-occurrence matrix
HAI	hepatic artery infusion
IH	intensity histogram
LBP	local binary pattern
MAPE	mean absolute prediction error
RECIST	Response Evaluation Criteria in Solid Tumors
RLM	run-length matrix

References:

1. Society AC (2016) Cancer facts and figures 2016. American Cancer Society Atlanta
2. Siegel RL, Miller KD, Jemal A (2015) Cancer statistics, 2015. CA Cancer J Clin 65:5–29 [PubMed: 25559415]
3. Manfredi S, Lepage C, Hatem C, Coatmeur O, Faivre J, Bouvier AM (2006) Epidemiology and management of liver metastases from colorectal cancer. Ann Surg 244:254–259 [PubMed: 16858188]
4. Amri R, Bordeianou LG, Sylla P, Berger DL (2015) Variations in Metastasis Site by Primary Location in Colon Cancer. J Gastrointest Surg 19:1522–1527 [PubMed: 25933582]
5. Cunningham D, Humblet Y, Siena S et al. (2004) Cetuximab monotherapy and cetuximab plus irinotecan in irinotecan-refractory metastatic colorectal cancer. N Engl J Med 351:337–345 [PubMed: 15269313]
6. Saltz LB, Cox JV, Blanke C et al. (2000) Irinotecan plus fluorouracil and leucovorin for metastatic colorectal cancer. Irinotecan Study Group. N Engl J Med 343:905–914 [PubMed: 11006366]
7. Lehmann K, Rickenbacher A, Weber A, Pestalozzi BC, Clavien PA (2012) Chemotherapy before liver resection of colorectal metastases: friend or foe? Ann Surg 255:237–247 [PubMed: 22041509]
8. Tomlinson JS, Jarnagin WR, DeMatteo RP et al. (2007) Actual 10-year survival after resection of colorectal liver metastases defines cure. J Clin Oncol 25:4575–4580 [PubMed: 17925551]
9. Eisenhauer EA, Therasse P, Bogaerts J et al. (2009) New response evaluation criteria in solid tumours: revised RECIST guideline (version 1.1). Eur J Cancer 45:228–247 [PubMed: 19097774]
10. Chun YS, Vauthey JN, Boonsirikamchai P et al. (2009) Association of computed tomography morphologic criteria with pathologic response and survival in patients treated with bevacizumab for colorectal liver metastases. JAMA 302:2338–2344 [PubMed: 19952320]
11. Piessevaux H, Buyse M, Schlichting M et al. (2013) Use of early tumor shrinkage to predict long-term outcome in metastatic colorectal cancer treated with cetuximab. J Clin Oncol 31:3764–3775 [PubMed: 24043732]
12. Suzuki C, Blomqvist L, Sundin A et al. (2012) The initial change in tumor size predicts response and survival in patients with metastatic colorectal cancer treated with combination chemotherapy. Ann Oncol 23:948–954 [PubMed: 21832285]
13. Kim DH, Kim SH, Im SA et al. (2012) Intermodality comparison between 3D perfusion CT and 18F-FDG PET/CT imaging for predicting early tumor response in patients with liver metastasis after chemotherapy: preliminary results of a prospective study. Eur J Radiol 81:3542–3550 [PubMed: 22459347]
14. De Bruyne S, Van Damme N, Smeets P et al. (2012) Value of DCE-MRI and FDG-PET/CT in the prediction of response to preoperative chemotherapy with bevacizumab for colorectal liver metastases. Br J Cancer 106:1926–1933 [PubMed: 22596235]
15. Coenegrachts K, Bols A, Haspeslagh M, Rigauts H (2012) Prediction and monitoring of treatment effect using T1-weighted dynamic contrast-enhanced magnetic resonance imaging in colorectal liver metastases: potential of whole tumour ROI and selective ROI analysis. Eur J Radiol 81:3870–3876 [PubMed: 22944331]
16. Liang HY, Huang YQ, Yang ZX, Ying D, Zeng MS, Rao SX (2015) Potential of MR histogram analyses for prediction of response to chemotherapy in patients with colorectal hepatic metastases. Eur Radiol. 10.1007/s00330-015-4043-2
17. McNitt-Gray MF, Bidaut LM, Armato SG et al. (2009) Computed tomography assessment of response to therapy: tumor volume change measurement, truth data, and error. Transl Oncol 2:216–222 [PubMed: 19956381]
18. Land WH, Margolis D, Gottlieb R, Krupinski EA, Yang JY (2010) Improving CT prediction of treatment response in patients with metastatic colorectal carcinoma using statistical learning theory. BMC Genomics 11 Suppl 3:S15
19. Zhao B, Oxnard GR, Moskowitz CS et al. (2010) A pilot study of volume measurement as a method of tumor response evaluation to aid biomarker development. Clin Cancer Res 16:4647–4653 [PubMed: 20534736]

20. Lambin P, Rios-Velazquez E, Leijenaar R et al. (2012) Radiomics: extracting more information from medical images using advanced feature analysis. Eur J Cancer 48:441–446 [PubMed: 22257792]
21. Ng F, Ganeshan B, Kozarski R, Miles KA, Goh V (2013) Assessment of primary colorectal cancer heterogeneity by using whole-tumor texture analysis: contrast-enhanced CT texture as a biomarker of 5-year survival. Radiology 266:177–184 [PubMed: 23151829]
22. Lubner MG, Stabo N, Lubner SJ et al. (2015) CT textural analysis of hepatic metastatic colorectal cancer: pre-treatment tumor heterogeneity correlates with pathology and clinical outcomes. Abdom Imaging 40:2331–2337 [PubMed: 25968046]
23. Kemeny NE, Melendez FD, Capanu M et al. (2009) Conversion to resectability using hepatic artery infusion plus systemic chemotherapy for the treatment of unresectable liver metastases from colorectal carcinoma. J Clin Oncol 27:3465–3471 [PubMed: 19470932]
24. D'Angelica MI, Correa-Gallego C, Paty PB et al. (2015) Phase II trial of hepatic artery infusional and systemic chemotherapy for patients with unresectable hepatic metastases from colorectal cancer: conversion to resection and long-term outcomes. Ann Surg 261:353–360 [PubMed: 24646562]
25. Wolf PS, Park JO, Bao F et al. (2013) Preoperative chemotherapy and the risk of hepatotoxicity and morbidity after liver resection for metastatic colorectal cancer: a single institution experience. J Am Coll Surg 216:41–49 [PubMed: 23041049]
26. Fong Y, Fortner J, Sun RL, Brennan MF, Blumgart LH (1999) Clinical score for predicting recurrence after hepatic resection for metastatic colorectal cancer: analysis of 1001 consecutive cases. Ann Surg 230:309–318; discussion 318–321 [PubMed: 10493478]
27. Allen PJ, Nissan A, Picon AI et al. (2005) Technical complications and durability of hepatic artery infusion pumps for unresectable colorectal liver metastases: an institutional experience of 544 consecutive cases. J Am Coll Surg 201:57–65 [PubMed: 15978444]
28. Haralick RM, Shanmuga K, Dinstein I (1973) Textural Features for Image Classification. Ieee Transactions on Systems Man and Cybernetics Smc 3:610–621
29. Soh LK, Tsatsoulis C (1999) Texture analysis of SAR sea ice imagery using gray level co-occurrence matrices. Ieee Transactions on Geoscience and Remote Sensing 37:780–795
30. Clausi DA (2002) An analysis of co-occurrence texture statistics as a function of grey level quantization. Canadian Journal of Remote Sensing 28:45–62
31. Tang XO (1998) Texture information in run-length matrices. Ieee Transactions on Image Processing 7:1602–1609 [PubMed: 18276225]
32. Pietikainen M, Zhao GY, Hadid A, Ahonen T (2011) Local Binary Patterns for Still Images. Computer Vision Using Local Binary Patterns 40:13–47
33. Mehta R, Egiazarian KO (2013) Rotated Local Binary Pattern (RLBP)-Rotation Invariant Texture DescriptorICPRAM, pp 497–502
34. Buczkowski S, Kyriacos S, Nekka F, Cartilier L (1998) The modified box-counting method: Analysis of some characteristic parameters. Pattern Recognition 31:411–418
35. Al-Kadi OS, Watson D (2008) Texture analysis of aggressive and nonaggressive lung tumor CE CT images. Ieee Transactions on Biomedical Engineering 55:1822–1830 [PubMed: 18595800]
36. Chakraborty J, Rangayyan RM, Banik S, Mukhopadhyay S, Desautels JEL (2012) Statistical measures of orientation of texture for the detection of architectural distortion in prior mammograms of interval-cancer. Journal of Electronic Imaging 21
37. Yang XF, Tridandapani S, Beitler JJ et al. (2012) Ultrasound GLCM texture analysis of radiation-induced parotid-gland injury in head-and-neck cancer radiotherapy: An in vivo study of late toxicity. Medical Physics 39:5732–5739 [PubMed: 22957638]
38. Banik S, Rangayyan RM, Desautels JE (2013) Measures of angular spread and entropy for the detection of architectural distortion in prior mammograms. Int J Comput Assist Radiol Surg 8:121–134 [PubMed: 22460365]
39. Ojala T, Pietikainen M, Harwood D (1996) A comparative study of texture measures with classification based on feature distributions. Pattern Recognition 29:51–59

40. Costa AF, Humpire-Mamani G, Traina AJM (2012) An efficient algorithm for fractal analysis of texturesGraphics, Patterns and Images (SIBGRAPI), 2012 25th SIBGRAPI Conference on. IEEE, pp 39–46

41. Chakraborty J, Rangayyan RM, Banik S, Mukhopadhyay S, Desautels JEL (2012) Detection of Architectural Distortion in Prior Mammograms Using Statistical Measures of Orientation of Texture. Medical Imaging 2012: Computer-Aided Diagnosis 8315

42. Chakraborty J, Midya A, Mukhopadhyay S, Sadhu A (2013) Automatic Characterization of Masses in Mammograms. Proceedings of the 2013 6th International Conference on Biomedical Engineering and Informatics (Bmei 2013), Vols 1 and 2:111–115

43. Soussan M, Orlhac F, Boubaya M et al. (2014) Relationship between tumor heterogeneity measured on FDG-PET/CT and pathological prognostic factors in invasive breast cancer. PLoS One 9:e94017 [PubMed: 24722644]

44. Henderson S, Purdie C, Michie C et al. (2017) Interim heterogeneity changes measured using entropy texture features on T2-weighted MRI at 3.0 T are associated with pathological response to neoadjuvant chemotherapy in primary breast cancer. Eur Radiol 27:4602–4611 [PubMed: 28523352]

45. Goere D, Deshaies I, de Baere T et al. (2010) Prolonged survival of initially unresectable hepatic colorectal cancer patients treated with hepatic arterial infusion of oxaliplatin followed by radical surgery of metastases. Ann Surg 251:686–691 [PubMed: 20224373]

46. Zacharias AJ, Jayakrishnan TT, Rajeev R et al. (2015) Comparative Effectiveness of Hepatic Artery Based Therapies for Unresectable Colorectal Liver Metastases: A Meta-Analysis. PLoS One 10:e0139940 [PubMed: 26448327]

47. Karanicolas PJ, Metrakos P, Chan K et al. (2014) Hepatic arterial infusion pump chemotherapy in the management of colorectal liver metastases: expert consensus statement. Curr Oncol 21:e129–136 [PubMed: 24523610]

48. Mise Y, Zimmitti G, Shindoh J et al. (2015) RAS mutations predict radiologic and pathologic response in patients treated with chemotherapy before resection of colorectal liver metastases. Ann Surg Oncol 22:834–842 [PubMed: 25227306]

Key points

- Colorectal liver metastases (CRLM) are downsized with chemotherapy
- Predicting the patients that will respond to chemotherapy is challenging
- Heterogeneity and enhancement patterns of CRLM can be measured with quantitative imaging
- Prediction model constructed that predicts volumetric response with 20% error
- Quantitative imaging holds promise to better select patients for specific treatments

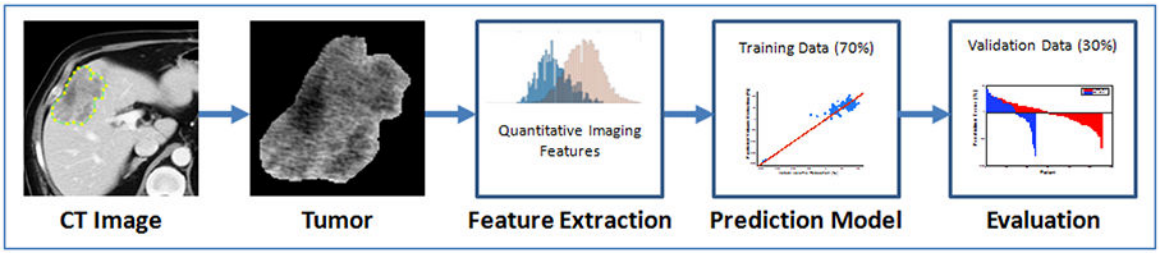

Figure 1.

Quantitative imaging workflow for prediction of tumor response. On the pre-treatment CT image, segmentation is performed to outline the index tumor. Quantitative imaging features are extracted from this region. 70% of the data (n=110) was used to construct a prediction model, and 30% (n=47) of the data reserved for validation.

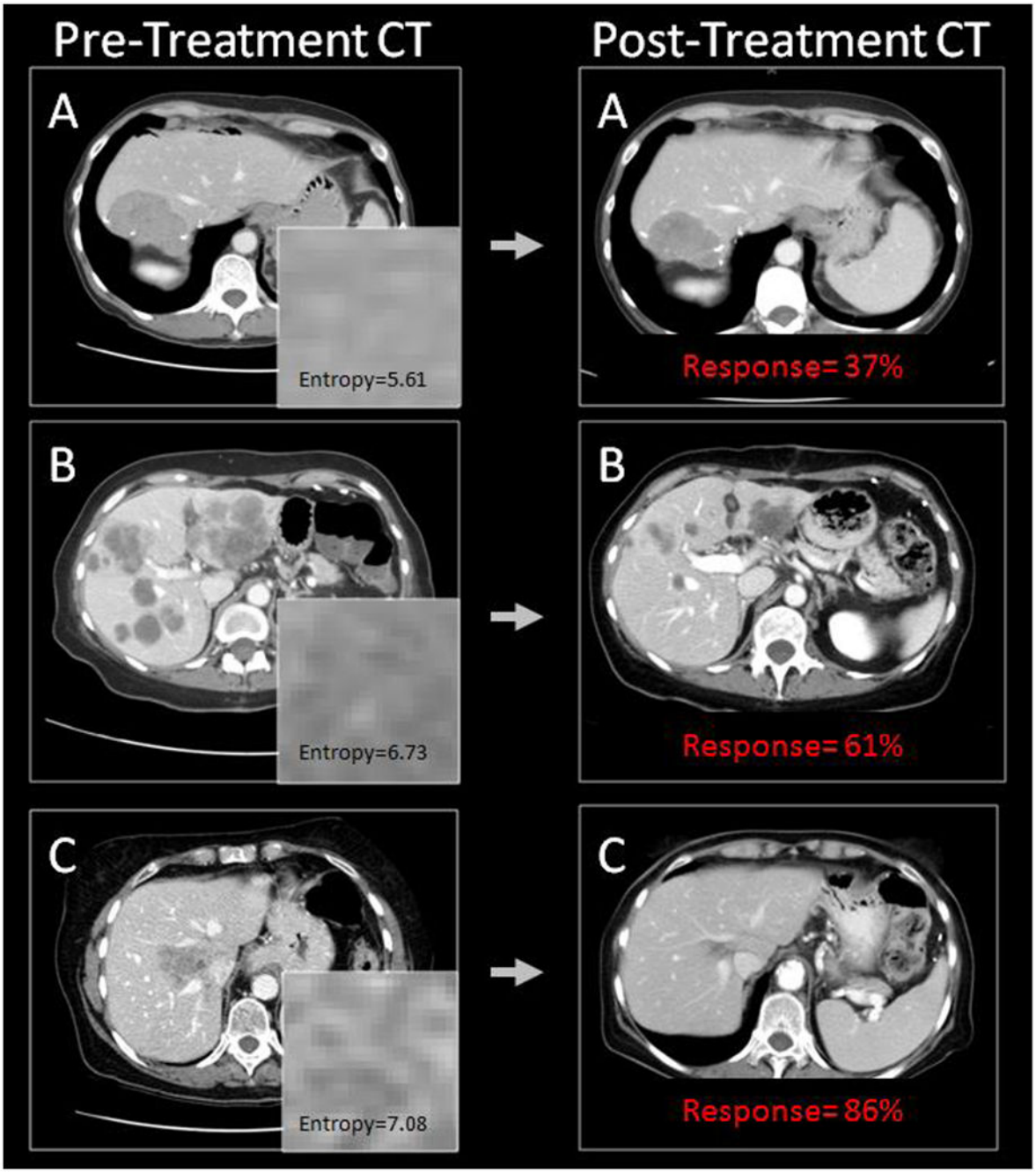

Figure 2.

Representative CT images of 3 patients. Entropy was one of the 30 selected features in the final multivariate regression model and represents pixel randomness in a gray-scale image. Higher entropy values were associated with improved response.

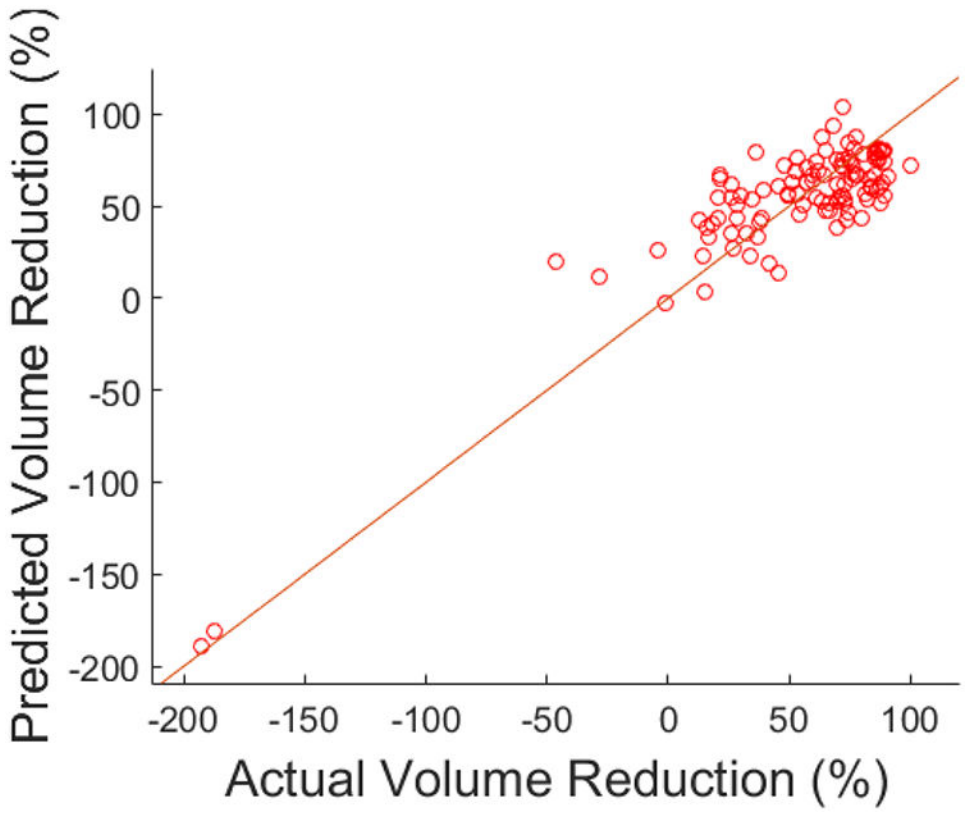

Figure 3a.
Scatter plot for training data, predicted versus actual volume reduction.

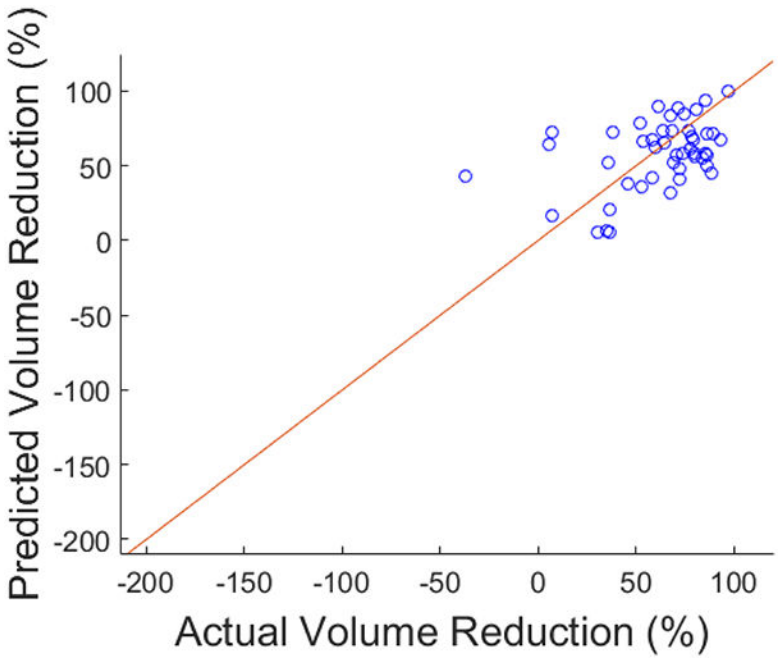

Figure 3b.
Scatter plot for test data, predicted versus actual volume reduction.

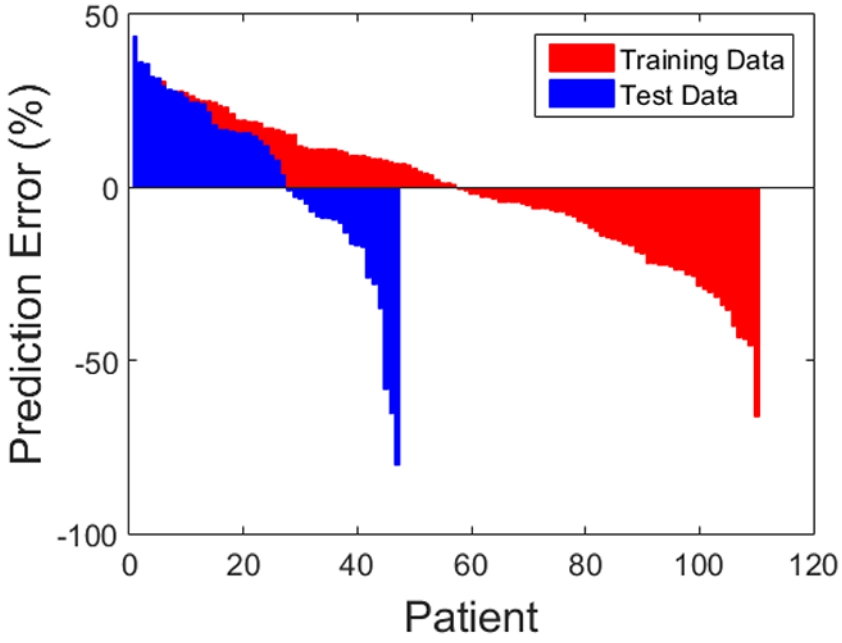

Figure 3c.
Waterfall plot of individual training and test set error.

Table 1.

Clinical factors associated with response, and comparison of training and validation set.

	1a. Comparison of volumetric response according to clinical factors				1b. Comparison of Training and Validation set		
	All Patients				Training	Validation	
Demographics/Characteristic	Total, Value=157	Actual Volume Reduction	p		Value=110	Value=47	p
	N (%)	Median (Minimum, Maximum)			N (%)	N (%)	
Age			**0.007**				0.107
≤60 years old	98 (62)	−62.7% (−93.4, +192.7)			64 (58)	34 (72)	
>60 years old	59 (38)	−73.6% (−100.0, +187.4)			46 (42)	13 (28)	
Sex			0.375				0.164
Male	90 (57)	−67.9% (−97.2,+46.0)			59 (54)	31 (66)	
Female	67 (43)	−64.7% (−100.0, +192.7)			51 (46)	16 (34)	
Site of Primary			0.082				0.807
Colon	135 (86)	−69.4% (−100.0, +187.4)			95 (86)	40 (85)	
Rectum	22 (14)	−47.8% (−88.8, +192.7)			15 (14)	7 (15)	
Synchronous	133(85)	−66.8% (−100.0, +192.7)	0.671		93 (85)	40 (85)	1.000
Bilobar	132(84)	−66.8% (−100.0, +37.4)	0.608		92 (84)	40 (85)	1.000
Multiple Lesions	141 (90)	−66.8% (−100.0, +37.4)	0.655		98 (89)	43 (91)	0.779
Node-positive primary	114(73)	−67.9% (−97.3, +192.7)	0.881		80 (73)	34 (72)	1.000
Largest tumor >5cm	65 (41)	−70.0% (−91.1, −13.0)	0.590		43 (39)	22 (47)	0.382
CEA >200	38 (24)	−67.0% (−88.8, −7.4)	0.898		21 (19)	17 (36)	**0.040**
Clinical Risk Score, n=152			0.403				0.902
0–2	34 (22)	−65.6% (−100.0, +187.4)			24 (23)	10 (22)	
>3	118 (78)	−68.3% (−97.3, +37.4)			82 (77)	36 (78)	
T reatment Strategy			**0.001**				0.917
HAI, chemotherapy naive	43 (27)	−74.1% (−97.3, −21.0)			31 (28)	12 (26)	
HAI, previous treatment	60 (38)	−61.1% (−93.4, +37.4)			41 (37)	19 (40)	
Systemic only, chemotherapy naive	54 (34)	−65.6% (−100.0, +192.7)			38 (35)	16 (34)	
Systemic Chemotherapy Regimens *			**0.001**				0.483
Oxaliplatin	40 (25)	−54.8% (−100.0, +192.7)			28 (25)	12 (26)	
Irinotecan	50 (32)	−63.0% (−93.4, +37.4)			38 (35)	12 (26)	
Oxaliplatin and Irinotecan	67 (43)	−72.6% (−97.3, −15.5)			44 (40)	23 (49)	
Bevacizumab	39 (25)	−52.5% (−93.4, +46.0)	**0.005**		24 (22)	15 (32)	0.226
KRAS mutational status			**0.006**				0.092
Mutant	30 (19)	−55.4% (−89.4, +37.4)			22 (20)	8 (17)	
Wild type	70 (45)	−74.2% (−97.3, +46.0)			54 (49)	16 (34)	
Unknown	57 (36)	−64.7% (−100.0, +192.7)			34 (31)	23 (49)	

Abbreviations: CEA, carcinoembryonic antigen; KRAS, Kirsten rat sarcoma viral oncogene homolog; FU, Fluorouracil

* Note: all patients that received both Oxaliplatin and Irinotecan had concurrent HAI

Table 2.

Selected Features for Model

RECIST Slice Normalized Intensity Feature (5 features) Skewness Entropy	**LBP (127 features)** L4 (frequency of 3rd bin of ULBP) L9 (frequency of 8th bin of ULBP) L13 (frequency of 12th bin of ULBP) L19 (frequency of 18th bin of ULBP) L20 (frequency of 19th bin of ULBP) L25 (frequency of 24th bin of ULBP) L27 (frequency of 26th bin of ULBP) L31 (frequency of 30th bin of ULBP) L32 (frequency of 31st bin of ULBP) L40 (frequency of 39th bin of ULBP) L51 (frequency of 50th bin of ULBP) L52 (frequency of 51th bin of ULBP) L53 (frequency of 52nd bin of ULBP) L55 (frequency of 54th bin of ULBP) L62 (frequency of 2nd bin of RI-LBp) L95 (4th frequency co-efficient of RI-ULBP Fourier spectrum) L103 (12th frequency co-efficient of RI-ULBP Fourier spectrum) L113 (22nd frequency co-efficient of RI-ULBP Fourier spectrum)
RECIST Slice Shape Feature (7 features) Compactness	
Intensity features at original Scale (5 features) Entropy	
GLCM (19 features) G7 (Sum variance)	
RLM (11 features) R8 (Short run low gray-level emphasis)	**FD (54 features)** [36,37] F51 Maximum of lacunarity of FD F54 Average of lacunarity of FD
Intensity features at normalized scale (5 features) I3 (Skewness)	**ACM1 (19 features)** ACM15 (Inverse difference moment) ACM17 (Sum variance)
	ACM2 (19 features) ACM217 (Cluster prominence)

Table 3.

Prediction model results from 70/30 training (n=110) and test (n=47) sets.

	Value	Training MAPE	Training R^2	Test MAPE
All Patients	N=157 (110/47)	16.5%	0.774	21.5%
HAI	N=103 (72/31)	14.8%	0.547	19.6%
Systemic	N=54 (38/16)	19.8%	0.844	25.1%

MAPE: mean absolute prediction error